KSME

Springer

Journal of Mechanical Science and Technology 39 (4) 2025

Original Article
DOI 10.1007/s12206-025-0311-5

Keywords:
· 316L stainless steel
· Heat treatment
· Biocorrosion
· Hardness

Correspondence to:
Şakir Altınsoy
sakir.altinsoy@yeniyuzyil.edu.tr

Citation:
Altınsoy, Ş., Kaftan, W. S. S., Üllen, N. B., Kızılbey, K. (2025). Investigation of corrosion behavior in SBF, hank, and ringer solutions of heat-treated 316L stainless steel using different cooling media. Journal of Mechanical Science and Technology 39 (4) (2025) 1835~1846. http://doi.org/10.1007/s12206-025-0311-5

Received May 10th, 2024
Revised November 1st, 2024
Accepted December 14th, 2024

† Recommended by Editor
Jun-Hyub Park

© The Korean Society of Mechanical Engineers and Springer-Verlag GmbH Germany, part of Springer Nature 2025

Investigation of corrosion behavior in SBF, hank, and ringer solutions of heat-treated 316L stainless steel using different cooling media

Şakir Altınsoy[1], Wasan Shareef Sadeq Kaftan[2], Nuray Beköz Üllen[3] and Kadriye Kızılbey[4]

[1]Faculty of Engineering and Architecture, Istanbul Yeni Yuzyil University, Istanbul 34000, Turkey, [2]Medical Laboratory Techniques, Al-Hikma University College, Baghdad 10013, Iraq, [3]Faculty of Engineering, Istanbul University-Cerrahpasa, Istanbul 34000, Turkey, [4]Faculty of Engineering and Natural Sciences, Acibadem University, Istanbul 34000, Turkey

Abstract SS316L is used in many areas, from the food industry to nuclear power plants, owing to its excellent corrosion resistance and mechanical strength. In this study, the effects of phase transformations in the microstructure on hardness, surface quality, and corrosion properties in simulated body fluid, Hank's, and Ringer's solutions were investigated by applying heat treatment at different cooling media to SS316L. For this purpose, surface characterization and electrochemical corrosion tests of heat-treated parts were carried out. The roughness of the steel surface was increased after heat treatment. The cooling media and the corrosive environment significantly influenced the mechanical properties and corrosion resistance. Results illustrated that heat treatment altered the microstructure, resulting in improved mechanical properties and corrosion resistance. The corrosion resistance of samples heat-treated in air and oil media was better. The heat-treated sample in oil exhibited a low passive current density, whereas the current density of those treated in water was highest in all solutions. Corrosive environments increased weight loss and surface roughness.

1. Introduction

Material improvement has become a significant research focus with advancing technology. The development of technology provides the products required to improve the quality of life. The technology develops the effect of concepts such as time, cost, and quality [1]. Stainless steels are widely preferred as building materials today, mainly because of their superior corrosion resistance and mechanical properties [2–4]. The level of nickel above 8 % in stainless steels that are classified under five categories as per their microstructure stabilizes austenite at room temperature; these stainless steels are classified as austenitic [5]. Such austenitic stainless steels are the most extensively used stainless steels, of which SS304 and SS316L are the most widely found types. SS316L contains 12 %–25 % chromium, 8 %–25 % nickel, and 2.2 % molybdenum, and it finds areas of use in chloride media where SS304 falls short [6–8]. Austenitic stainless steels are extensively used in petrochemistry, medical, hydrometallurgy, nuclear industries, and numerous other traditional industries given their perfect mechanical properties, good weldability, and corrosion resistance. However, their friction coefficient, hardness, and wear resistance are generally inadequate. Heat treatment and coating methods are used to overcome such problems [9, 10]. SS316L is broadly used in thermal, nuclear, medical, and petrochemical industries and other domains owing to its long-term operation capacity under high temperatures and harsh ambient conditions that may cause damage such as abrasion [11–14]. In applications, the metals are frequently exposed to air, steam, water, and other chemicals. Because of the contact between metals and their environment, chemical interactions, such as metal corrosion, occur on the surface. Metallic materials operating in corrosive

environments, particularly low-carbon stainless steel S316L, may lead to critical consequences due to corrosion cracking. This study aims to investigate the corrosion behavior of SS316L stainless steel in various corrosive environments.

Medical implants made of SS316L stainless steel are extensively and successfully used in various orthopedic implementations, with advantages such as better mechanical properties than bones, ease of manufacture, and availability at a low cost [15–18]. However, research has shown that SS316L is prone to corrosion when used in vivo, leading to the release of metal ions (e.g., Fe, Cr, and Ni). Many metallic materials operating in corrosive environments can be subjected to mechanical stresses. Especially, low-carbon stainless steels, which have been induced to harden owing to their manufacturing processes, can have important consequences in terms of stress corrosion cracking behavior in different corrosive environments. Understanding the environmental factors and mechanisms that promote stress corrosion cracking in such environments is of great importance. Thus, assessing the corrosion resistance of such materials in different environments and increasing such resistance are crucial. Heat treatments applied to such materials, along with the selection of suitable materials, are also important [15, 19–21]. The chromium oxide layer that forms as a passive film on the surface of stainless steel naturally expands, providing remarkable corrosion resistance. Any material used in a biological system must be inert and devoid of harmful effects on the environment. When SS316L is implanted, its interaction with surrounding tissue influences its biocompatibility. This effect is linked to the material's ability to appropriately respond to the host for optimal function [17, 22]. Contact of implants with tissue and surface interactions between the implant and physiological orthopedic devices present a common issue. Such interactions reason abrasion, corrosion, and wear, resulting in negative effects on the patient, and they also lead to the rejection of tissue or fluids surrounding the implant surface. The main prerequisites in the selection of biomaterials are their biocompatibility with the tissue, lack of toxicity, and corrosion and wear resistance [23]. Heat treatment affects the grain size within the steel's microstructure, altering its corrosion behavior. Additionally, heat treatment influences biocorrosion and hardness through the formation of oxide films on the surface.

The oxide layer on the surface of stainless steel consists of two layers: an outer layer characterized by Fe_2O_3 and NiO and an inner layer characterized by Cr_2O_3 [17, 24]. Corrosion resistance relies on the formation of a dense and protective Cr_2O_3 layer (a thin passive surface). With the break of such a layer, the steel is regionally exposed to corrosive attack, and the corrosion continues to proceed in the area that becomes active in this manner. As a result, corrosion types such as stress corrosion, intercrystalline corrosion, pitting, and crevice corrosion are observed. Advancements in materials engineering have the potential to enhance the corrosion resistance of metals through the application of suitable operations, increase their biocompatibility, and enable the use of alloys in medicine, dentistry, and orthopedics. The corrosion behavior can be altered by changing the microstructure of the materials. Heat treatment involves heating and cooling operations to modify the properties of metals and alloys in their solid form. The heating and cooling operations are performed in a controlled manner. This process increases the mobility of atoms, allowing them to move into new positions. Through heat treatment, new properties can be provided for the materials through hardness, strength, resistance to impacts, and changes in chemical composition and crystal structure [25, 26]. Corrosion of stainless steel implants is an electrochemical process that binds to the surface and causes changes in the body's response. The release of ions such as Ni and Cr is the result of such an operation, and it negatively affects the body's reaction to the implant. According to literature, natural Cr^{3+}, Fe^{2+}, and Ni^{2+} ion concentrations in the body may severely impair tissue function and cause significant health problems. For that reason, the primary issue to address in implant design is material corrosion. The identification of biological variables affecting corrosion is also a must. Scientific in vitro and in vivo studies on the corrosion behavior of metal implants were performed with the use of different simulated fluids [22]. Manufacturers need to know the effect of cooling media to optimize the corrosion resistance, and this study can be applied in the industrial scene. Numerous studies have been conducted on the microstructural and mechanical properties of SS316L. However, studies on the detailed investigation of the relationship between heat treatment and corrosion are limited. Filling this gap in the literature is important for increasing the use of SS316L in the biomedical field. This study aims to examine and compare the effect of heat treatment on the corrosion resistance and surface property of SS316L in different corrosive environments such as simulated body fluid (SBF), Hank's, and Ringer's solutions. Mechanical tests were performed to determine which heat treatment process provides the optimum properties.

2. Experimental details

2.1 Materials and heat treatment process

In this study, SS316L steel rods with a diameter of 30 mm, obtained from Birçelik Stainless Steel Trade Inc., were used. The chemical composition of the SS316L austenitic stainless steel used in the experimental study is given in Table 1.

Orthogonal surface turning treatment of SS316L pieces was performed on a CNC counter produced by YouJi Machine Industrial Co., Ltd. A mixture of 5 % ESTRA metalworking fluid and 95 % water was used in all treatments. The workpieces were prepared in dimensions of Ø 25×2.5 mm with a cutting speed of 50 m/min, a feed rate of 0.10 mm/dev, and a cutting depth of 0.4 mm. For the attainment of the required toughness, hardness, and strength, heat treatment was applied to the samples to be used in the experiment in the vacuum furnaces of Censaş Heat Treatment Company. The cooling medium selection criteria were determined in accordance with industry standards (in consultation with the heat treatment company)

Table 1. Chemical composition of SS316L material with percentage (%) used in the experiments.

Element	C	Mn	Si	Cr	Ni	Cu	N	P	S	Mo	Fe
Percentage (%) in SS316L	0.017	1.29	0.416	16.60	10.06	0.427	0.037	0.031	0.023	2.503	Remainder

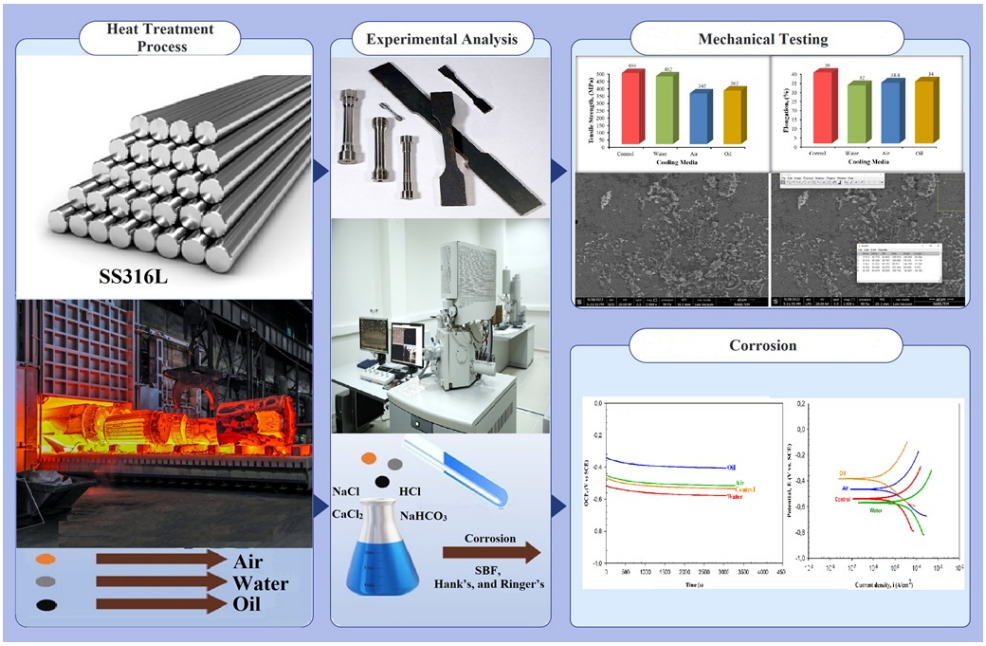

Fig. 1. Schematic view of experimental steps.

and literature research. The heat treatment process was done by standing at 450 °C for 40 min before normalization. The samples were placed in an oven, reaching 1100 °C after normalization in 30 min of processing time. The vacuum environment inside the furnace was utilized to prevent oxide layer formation on the sample surfaces during heat treatment. Then, the samples were cooled in three different media: water, air, and oil. The schematic view of the experimental steps is given in Fig. 1.

2.2 Mechanical tests

Rockwell HRB hardness measurements of the samples were performed in three different areas of each sample by using an Innovatest-branded Versuz 750 CCD model device, and the average of such measurements was calculated. The tensile strength test of the pull rods prepared in the standard direction was performed using a Zwick & Instron Model 3367 tensile test device. Three tests were performed for each test parameter. The tensile test was intended to determine the effect of cooling media on mechanical properties.

2.3 SEM-EDS analysis

Before and after the heat treatment, the effects of cooling media and heat treatment parameters on morphology and grain size were examined by FEI-branded QUANTA FEG 250 model SEM/EDS microanalysis at the NABİLTEM Center of the Central Research Laboratory of the Tekirdağ Namık Kemal University. ImageJ software was used for grain size analysis.

2.4 Electrochemical corrosion tests

Electrochemical corrosion studies were performed in SBF, Hank's, and Ringer's solutions simulated via a computer-controlled potentiostat (Interface 1000 Potentiostat, Gamry, USA). The chemical compositions of the SBF, Hank's, and Ringer's solutions are listed in Table 2. A glass corrosion test cell with a volume of 1000 ml was used. A three-electrode high-density graphite rod was adopted as the counter electrode, the saturated calomel electrode as the reference electrode, and the sample as the working electrode. Data analysis was performed through computer software (Framework and Echem Analyst Gamry). Samples were prepared by being cut and then coated with epoxy resin. Then, they were connected via copper wire. All tests were performed at room temperature. Before electrochemical corrosion tests, the open circuit potential (OCP) values of the samples were measured. The OCP level was measured at 2–3 h intervals until the stabilization of the OCP value. The OCP value was deemed stable when the OCP curve had an asymptotically stable area. Tafel curves were created by polarizing the samples from −250 mV to +250 mV (against the SCE) regarding the OCP at a scanning rate of 1.0 mV/s.

Table 2. Chemical composition of SBF, Hank's, and Ringer's solutions (g/L) [27, 28].

Components	SBF solution	Hank's solution	Ringer's solution
NaCl	12.053	8.0	9.0
$NaHCO_3$	0.533	0.35	0.20
KCl	0.338	0.40	0.40
$K2HPO_4{\cdot}_3H_2O$	0.347	-	-
$MgCl_2{\cdot}6H_2O$	0.467	0.10	-
1 M HCl	50 ml	-	-
$CaCl_2$	0.438	0.14	0.25
Na_2SO_4	0.108	-	-
$C_4H_{11}NO_3$ (Tris)	9.177	-	-
1 M HCl	8.5 ml	-	-
$Na_2HPO_4.2H_2O$	-	0.06	-
KH_2PO_4	-	0.60	-
$MgSO_4.7H_2O$	-	0.06	-
Glucose	-	1.0	-

2.5 Surface roughness measurements

The surface roughness values (Ra) of untreated, heat-treated, and exposed SS316L surfaces to different corrosive environments were measured. The average surface roughness changes of heat-treated parts before and after corrosion were evaluated using Mitutoyo's Surftest SJ-210 model instrument to explain the corrosion phenomenon. The mean Ra values were calculated by making five measurements.

3. Results and discussion

3.1 Mechanical test results

Most metallic materials operating in aggressive environments are subjected to mechanical stresses. These mechanical stresses can come from the environment where the material works, as well as residual stresses caused by manufacturing methods such as welding and machining and plastic deformation of the materials. One of the most important data in determining the life cycle of the elements operating in such environments is the damage to the material due to the combination of stress, corrosive environment, and corrosion-sensitive material factors [29, 30]. Corrosion presents a significant risk to biometallic structures due to mass loss. Heat treatment causes microstructural changes in unstabilized stainless steels and may decrease corrosion resistance.

Temperature allows chromium carbide precipitation with the decrease in chromium content at grain boundaries. Chromium content is the determining factor for the corrosion resistance level [31, 32]. Therefore, optimizing the heat treatment process is important. In this paper, the effect of cooling in different media (air, water, and oil) after heat treatment on mechanical properties is explained. Fig. 2 compares the hardness results after the heat treatment.

From the results in Fig. 2, the average hardness value of the

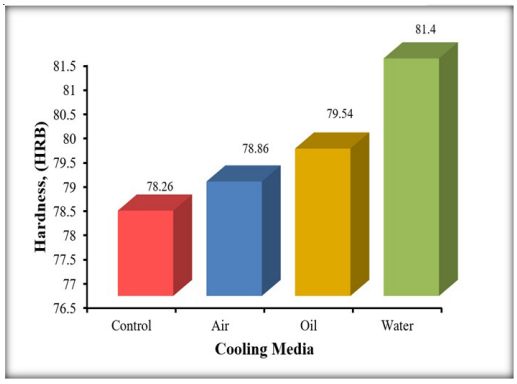

Fig. 2. Comparison of hardness results after heat treatment.

control sample increased from 78.26 HRB to 78.86, 79.54, and 81.40 HRB under air, oil, and water cooling media, respectively. A hardness increase of 1 % was measured between the air and control samples, 1 % between the oil and air samples, 2 % between the water and oil samples, 2 % between the oil and control samples, and 4 % between the water and control samples. The highest increase was measured between the water and control samples. The ferrite–austenite ratio in the untreated sample caused it to have a lower hardness value than it had in a balanced ratio [33, 34]. This circumstance may be explained with regard to the rate of ferrite in the microstructure. The ferrite in the control sample was at an austenite-balanced rate, and the hardness was found to be lower than that of the samples subjected to heat treatment [3]. The sigma phase in the water-cooled sample likely enhanced the hardness. Modifying the microstructure of stainless steel significantly increases corrosion resistance. Grain size is strongly modified by heat treatment to cause changes in mechanical, chemical, and surface properties based on phases, precipitates, austenite/martensite formation, changes in grain size, and defects [35].

The uniaxial tensile test is the most general testing method

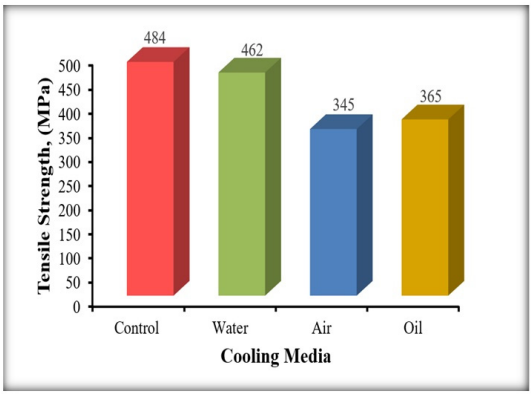

Fig. 3. Comparison of tensile strength after heat treatment.

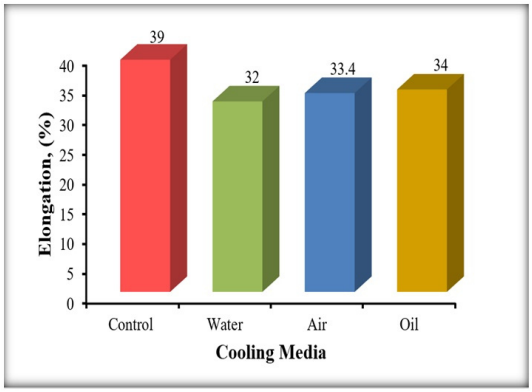

Fig. 4. Comparison of tensile strain after heat treatment.

applied for obtaining the mechanical properties of materials. With this test, Young's modulus, Poisson rate, yield strength, and strain properties can be determined. Fig. 3 shows the results of the tensile strength test. The percentage elongation values obtained from the tensile test of SS316L are graphically given in Fig. 4.

Based on the results of tensile strength given in Fig. 3, the average tensile strength value of the control samples decreased by 4.2 %, 24.5 %, and 28.4 % in water, oil, and air cooling media, respectively. In terms of elasticity, the water sample was 5 % lower than the control, the air sample was 40 % lower than the control, and the oil sample was 33 % lower than the control. The cooling medium affected the elasticity of the sample. The control sample exhibited the highest tensile strength. The equilibrium state in the ferrite–austenite ratio in the untreated sample kept the hardness value low and the tensile strength high [33]. From the strain results given in Fig. 4, the highest elongation ratio was obtained from the control sample. The elongation ratio decreased by 22 % between the control and water samples, by 17 % between the control and air samples, and by 15 % between the control and oil samples. The percentage elongation values obtained were in parallel with the results obtained from the tensile test. The tensile strength and ductility of the main material were higher than those of the materials subjected to heat treatment because of

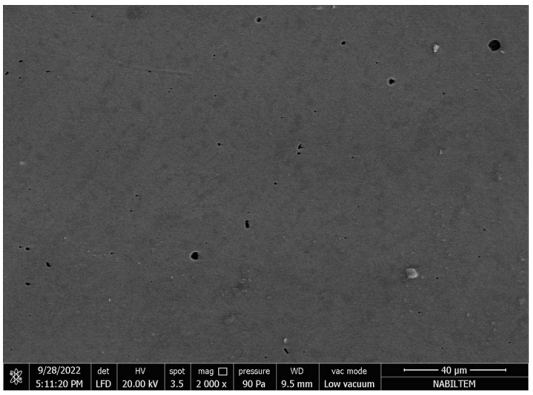

Fig. 5. SEM image of SS316L (control).

the decrease in elongation and tensile strength due to the coarsening of the microstructure induced by heat input [36–38].

3.2 SEM-EDS analysis results

The properties of metal materials may be checked by the grain size determined by microstructure. The progression of dislocations in materials ends with the formation of grain boundaries. Metal or nonmetal foreign waste may be present among the grain boundaries of commercially sold metal materials. Such residues dissolve with high-temperature heat treatment, and they enter the crystal structure of the base metal. As the boundary layers are eliminated in this manner, the grains with the same properties come side by side, and small grains go into large grains over time [39]. In this study, SEM images were obtained to determine the effects of heat treatment cooling media on the grain size of SS316L steel and its hardness and strength. Fig. 5 presents the SEM image of the untreated sample. SEM images of the heat-treated SS316L sample in water, oil, and air media are given in Figs. 6–8, respectively.

In Figs. 6–8, the dark gray areas indicate δ-ferrite, the light-colored areas show austenite (γ), and the black areas scattered at grain boundaries indicate the sigma (σ) phase. As shown in Fig. 5, no sigma phase exists in the microstructure of the untreated samples, whereas a sigma phase occurs in the sample after cooling in all three environments after heat treatment. In particular, the sigma phase is formed at the grain boundaries. From Fig. 6, the grain sizes of the pieces cooled under a water medium were small and homogenous given the insufficient time for grain growth. Through ImageJ software, the grain sizes were observed to be 15 µm on average. Fig. 7 depicts that the grain sizes of pieces cooled under an oil medium, i.e., approximately 23 µm, were 53 % larger than those of pieces under a water medium. In Fig. 8, the grain sizes in the inner structure of the sample cooled under an air medium were considerably different; some grains grew much faster than others. On the contrary, a homogenous distribution was observed in the other samples. The grain size of the pieces under the air medium, i.e., approximately 68 µm, was 196 % larger than that of the pieces under the oil medium because they had

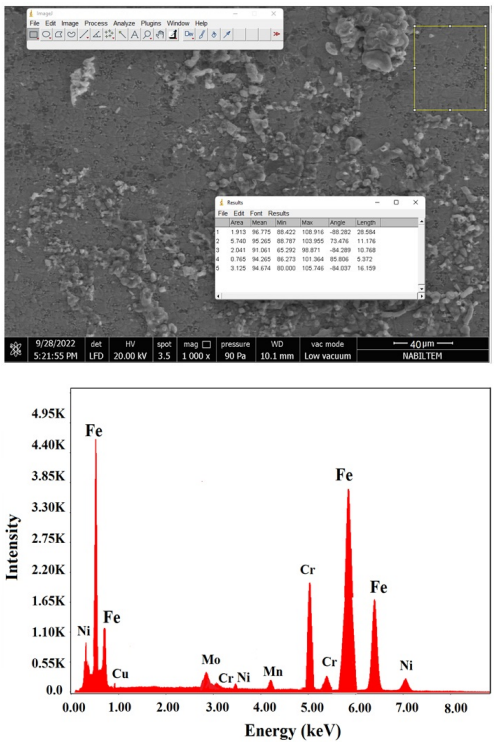

Fig. 6. SEM-EDS image of the heat-treated SS316L sample in water medium.

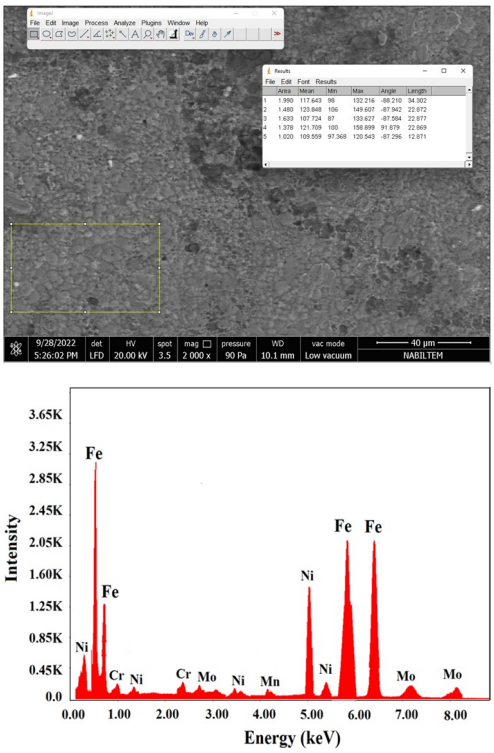

Fig. 7. SEM-EDS image of the heat-treated SS316L sample in oil medium.

adequate time for grain growth [40–43]. EDS results of heat-treated samples are also given in SEM images. The ferrite and

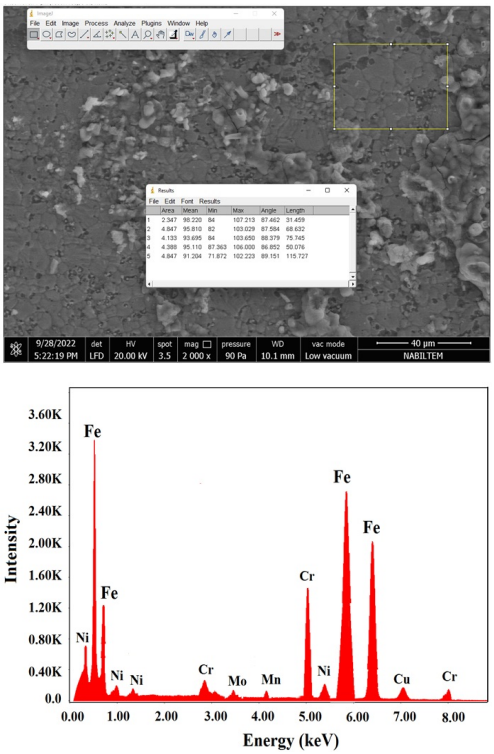

Fig. 8. SEM-EDS image of the heat-treated SS316L sample in air medium.

austenite phases contained Cr, Ni, and Mo. Cr and Mo ratios were higher in the ferrite phase (Fig. 6), whereas Ni was higher in the austenite phase (Fig. 8). The amount of Cr in the ferrite (Fig. 8) in the oven-cooled sample was lower than that in the water-cooled sample (Fig. 6) because the sigma phase tended to grow toward the ferrite phase [44]. That is, the sigma phase attracted the Cr element in the ferrite, which decreased the Cr ratio in the ferrite and increased the Cr ratio in the sigma phase (Fig. 8). SEM analyses showed that the subgrain structures changed from dislocation-rich subparticle boundaries to island-like cellular trace heat-treated structures in air and oil cooling media. This change would increase corrosion resistance owing to the elimination of dislocations and the homogenization of the composition [45]. Based on these results, corrosion resistance can be increased while optimizing the existing microstructure in cooling environments.

3.3 Electrochemical corrosion test results

The physicochemical interactions experienced by metallic materials with their environment are the cause of corrosion. Electrochemical corrosion is a chemical reaction that makes a metal lose its functionality through the release of metal ions as a result of the transfer of electrons from the zero-valent metal to an external electron [46]. Studies indicate that stainless steels are highly sensitive to localized corrosion types such as pitting, intergranular, and stress corrosion cracking and that these damage mechanisms can cause serious problems. Environmental factors and the production processes of materials

are extremely decisive in the formation of these damages [47]. Corrosive stress cracking and intergranular corrosion are critical corrosion processes that significantly affect the performance of austenitic stainless steel. Residual stresses created by the corrosive environment or low-value stresses occurring during operation may cause the protective oxide layer at these points to weaken and break, thus initiating crack formation by exposing the metal surface to corrosion. Stress corrosion cracking is a common mechanism that can occur in many different alloy systems and cause dramatic damage. The corrosion process of metals is largely affected by the environment where they are located. The amount of humidity in the environment, the acid–base condition, the ability of the air to pass oxygen or water from the environment, leakage currents, and various bacteria triggering and accelerating factors are determining aspects. Their resistance is determined on the basis of their chemical composition, passivation properties, heat treatment processes, and corrosive environment. In this study, the corrosion behavior of steel was examined in NaCl solutions of varying concentrations [48, 49]. Specifically, this study measured the corrosion properties of heat-treated stainless steel in SBF, Hank's, and Ringer's solutions with different NaCl contents. It investigated potential corrosion solutions by modifying the surface characteristics of SS316, cooled in different environments after heat treatment. The aim was to increase the corrosion resistance of SS316L, whose surface structure changes with heat treatment optimization, thus increasing the life and reliability of biomedical devices.

Fig. 9 presents the results of OCP measurements of the bare substrate and heat-treated surfaces with different cooling media. In particular, the results of OCP measurements for sample surfaces in the SBF, Hank's, and Ringer's solutions are displayed in Figs. 9(a)–(c), respectively. The main purpose of OCP measurement tests was to measure the potential of the materials against corrosion under the relevant test conditions and to determine the potential of forming a stable surface film. The OCP time graphs show that protective films formed on the surfaces under the cooling conditions, except that in the cooling treatment with water. While the OCP values of the control material were −0.50, −0.47, and −0.47 (V), such values moved toward −0.36, −0.34, and −0.36 (V) under the conditions of cooling with oil in the SBF, Hank's, and Ringer's solutions, respectively. In the air-cooling treatment, the OCP values increased up to −0.43, −0.45, and −0.40 (V) in the SBF, Hank's, and Ringer's solutions, respectively, compared with those of the control sample. By contrast, in the cooling treatment with water, the OCP values decreased to −0.54, −0.52, and −0.52 (V) in the SBF, Hank's, and Ringer's solutions, respectively. Fig. 10 illustrates the differences among these values for enhanced understanding. With reference to the SS316L control material, the corrosion resistance of the samples increased at rates of 28 %, 28 %, and 23 % in the SBF, Hank's, and Ringer's solutions, respectively, under the conditions of cooling with oil. Meanwhile, the OCP values increased at rates of 14 %, 4 %, and 15 % in the SBF, Hank's, and Ringer's solutions, respectively, between the air and control samples. On the contrary, the corrosion resistance between the water and control samples decreased by 8 %, 11 %, and 11 % in the SBF, Hank's,

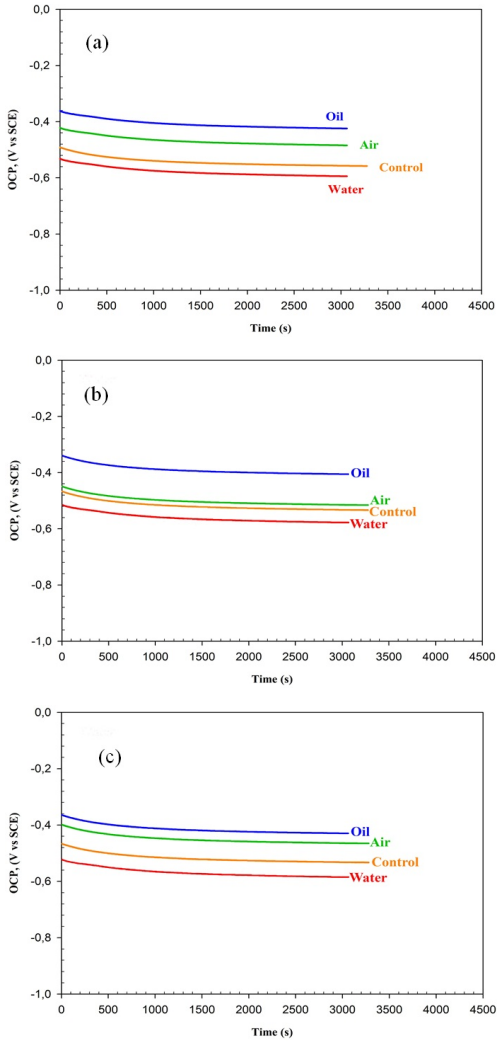

Fig. 9. OCP results in (a) SBF; (b) Hank's; (c) Ringer's solutions of untreated and heat-treated samples in different cooling media.

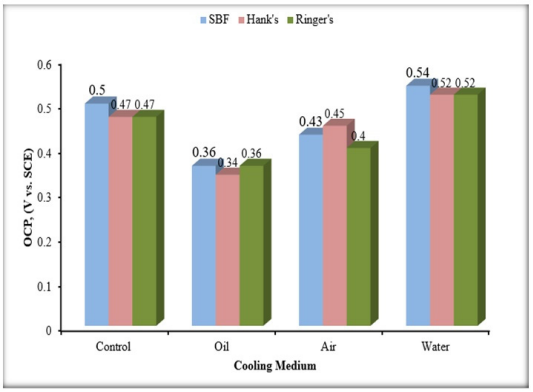

Fig. 10. Comparison of OCP values in different corrosion environments as a function of the heat treatment process.

and Ringer's solutions, respectively. In sum, the sample was resistant to corrosion at the rate of closeness of the line to zero as a result of OCP. Specifically, the corrosion resistance of SS316L cooled under an oil medium increased in all three solutions, which was attributed to the formation of a protective layer during cooling with oil. The results of SBF and Hank's solutions were better than the results of Ringer's solution [27, 28, 50–52].

The cooling medium in the heat treatment process affected the corrosion resistance of the material. The Cr released in the austenite matrix increased the corrosion resistance with the dissolution of carbides at austenitizing temperatures. The sample cooled in an oil environment had the highest OCP results. As a consequence of the changing heat treatment conditions, the different grain sizes of the metals and the concentrations in the two grains created a suitable environment for the initiation of corrosion at the grain boundaries [53]. Although the maximum amount of dissolved Cr was obtained by cooling in water, this sample showed the lowest corrosion resistance, which was related to the C released from the dissolved carbides. The lattice distortion increased because of the overincreased C content, leading to a defective passive layer [54]. In this study, the best cooling medium was determined as oil in all solutions, providing wear resistance and corrosion resistance. The microstructural analysis results revealed that the subgrain structures resembled island-like cellular trace heat-treated structures from dislocation-rich subgrain boundaries in air and oil media. This situation could lead to increased corrosion resistance due to the elimination of dislocations and the homogenization of the composition. Based on these results, heat treatment in these cooling media appears to be a sufficient post-treatment for SS316L to optimize the microstructure while increasing corrosion resistance. OCP values decreased with the increase in chloride concentration in the corrosion environment. According to the literature, the higher resistance of the ferrite phase to this chlorine-containing test medium than that of austenite can be explained as follows: the chlorine ions in the corrosion test solutions corroded austenite more. Arivazhagan et al. stated that corrosion in the sigma phase under reducing environments, such as hydrochloric acid, is on average 3 times higher than that in delta-ferrite [55]. The environment does not allow the transformation from active to passive behavior owing to the disrupting effect of chlorine ions on the passive cover. Corrosive ions triggered by the chloride environment induce pitting corrosion on the surface and initiate general corrosion in stainless steel materials. Stress corrosion cracking is a type of damage resulting from the combined effects of tensile stress and corrosive environment. It can be controlled in the presence of low chloride ions in the environment. However, even if corrosion does not start in this case, chloride ions initiate general corrosion under the passive layer on the surface, which results in general material loss [56, 57]. Abd Razak et al. investigated the corrosion behavior of AISI 304 stainless steel at varying NaCl concentrations and reported that H_2SO_4 caused a high amount of material loss because of the increase in intergranular corrosion with the increase in sulfur concentration at grain boundaries [31]. Ghosh and Kain explained that when a HCl solution is chosen as the corrosive environment, the dislocations on the shear plane weaken the atomic bonds by creating strain through chemical adsorption [58]. They stated that a sharp discontinuity occurs as a result of the decrease in surface energy, which accelerates corrosion.

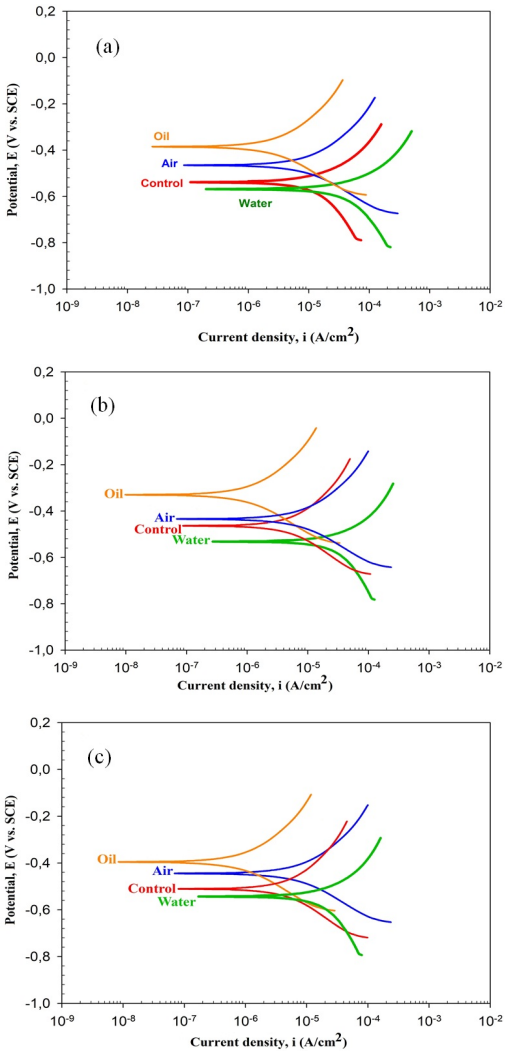

Fig. 11. Tafel curves in (a) SBF; (b) Hank's; (c) Ringer's solutions of untreated and heat-treated samples in different cooling media.

Fig. 11 shows the polarization curves of the bare substrate and heat-treated surfaces with different cooling media. Corrosion potentials (Ecorr) and corrosion current densities (Icorr) were obtained directly from the polarization curves via Tafel extrapolation. Smaller Icorr and larger Ecorr mean better corrosion resistance. Ecorr is a corrosion test that determines how well a surface is protected after heat treatment. Figs. 11(a)–(c) display the results of Tafel curves for sample surfaces in SBF, Hank's, and Ringer's solution, respectively. Under the method of cooling following heat treatment, a difference in corrosion resistance values of SS316L pieces was clearly observed. Low corrosion current followed by high corrosion potential is the

Table 3. Average surface roughness values after heat treatment and corrosion in various environments.

Heat treatment cooling medium	Average surface roughness (Ra, μm)			
	No-corrosion environment	Corrosive environment		
		SBF solution	Hank's solution	Ringer's solution
Water	1.456	1.855	1.643	1.546
Air	1.343	1.954	1.632	1.527
Oil	1.367	1.846	1.735	1.497

determinant of low corrosion rate and high wear resistance [59, 60]. According to the results of the Tafel curves obtained, potential changes toward the cathodic area were clear along with the change in cooling conditions. The tendency of the corrosion surface to passivate decreased through tension changes toward the cathodic area. Based on the examination of the values obtained, the corrosion resistances of all three solutions were lowest in the sample cooled with water. By contrast, the corrosion resistances were highest in the sample cooled with oil, followed by those in the sample cooled with air, and then those in the control sample not subjected to heat treatment. The results of the OCP values supported these findings [27, 28, 51].

The polarization behavior of the pieces in Ringer's solution following heat treatment showed a similar regime to that of the sample not subjected to heat treatment. The potentials of the pieces cooled in oil and air following heat treatment had more noble values. Especially following cooling in oil, the Tafel curves showed lower current density and high potential. This circumstance showed that the biometallic microstructure of SS316L, which changed following heat treatment, reflected lower ion release toward the electrolyte. The microstructure caused the change in electrochemical data and the spread of data in passive areas [61]. Differences in the microstructure of stainless steel significantly changed its corrosion resistance. Structural components such as grain size, macrostructural phases, macro- and microprecipitates, defects, and inclusions were changed by heat treatment, resulting in the formation of austenite–martensite, variations in grain size, and changes in mechanical, chemical, and surface properties [62]. Rapid cooling causes some of the austenite phase to transform into the martensite phase. The hardness of a metal due to quenching is a product of its elemental components and the heat treatment process. Previous research on the effect of heat treatment processes on the corrosion resistance of stainless steel has revealed mixed results. Lu et al. investigated changes in the microstructural properties and electrochemical behavior of plastic mold steel in a chloride solution due to heat treatment. The results showed that the corrosion resistance of quenched martensitic stainless steel increased with austenitizing temperature and decreased after tempering [63]. Isfahany et al. evaluated the effects of austenitization temperature and time on the mechanical characteristic, microstructure, and corrosion behavior of AISI 420 martensitic stainless steel. The results revealed that temperature exerted a significant effect on the mentioned properties of steel [64]. Lu et al. reported the effects of heat treatment process on the microstructural characteristics, hardness uniformity, surface roughness, and corrosion resistance of martensitic stainless steel and demonstrated that cooling in water reduced the corrosion resistance of the steel [63]. In this research, similar findings on the surface properties and corrosion resistance of SS316L in different corrosive environments and the effect of heat treatment with cooling in different media were obtained. These findings, being related to biocompatibility, are important in in vivo implants.

3.4 Surface roughness results

Surface roughness is an important parameter in the use of biomaterials as implants in biomedical fields. It affects the surface properties of biomaterials, such as hydrophilic and surface energy, and is critical in terms of corrosion resistance [65]. In this study, the average surface roughness values of the heat-treated parts with cooling in different media and the heat-treated parts corroded in different corrosive environments were obtained, as given in Table 3. The average surface roughness of the untreated SS316L part was 1.379 μm. In all environments, the surface had become rougher after heat treatment. The surface roughness value of the corroded sample surfaces in all coating conditions was higher than that of the non-heat-treated SS316L parts. Specifically, the surface roughness values of heat-treated parts cooled in water after corrosion in SBF, Hank's, and Ringer's solutions increased by 27 %, 13 %, and 6 %, respectively. The surface roughness values of heat-treated parts cooled in air after corrosion in SBF, Hank's, and Ringer's solutions increased by 45 %, 22 %, and 14 %, respectively. Similarly, the values of heat-treated parts cooled in oil after corrosion in SBF, Hank's, and Ringer's solutions increased by 35 %, 27 %, and 10 %, respectively. For corrosion studies, the parts were transferred to different electrolytes. According to the measured values, the surface roughness of all samples increased at the end of the corrosion test. In addition, the roughness value increased as the HCl ratio in the solution increased. This difference might be due to pit nucleation that developed at the initiation of stress corrosion cracks. In the surface grooves, the concentration of corrosive ions from the chloride environment created pits, and crack initiation was triggered in these peaks [66]. The increase in HCl concentration increased the overall corrosion damage and the crack

propagation rate. Therefore, the greatest corrosion in all samples occurred in the SBF solution with high HCl concentration. The increase in Ra values after the corrosion in the SBF solution supported this result. The results indicated that heat treatment and corrosive environments affected surface roughness, influencing corrosion resistance. Similar findings in the literature corroborate our results [67].

4. Conclusion

In this study, the effects of phase transformations in microstructure on tensile strength and hardness, surface quality, and corrosion behavior in corrosive environments were investigated by applying heat treatment with different cooling media to SS316L. The general results obtained are as follows:

- Secondary phases formed in the structure after heat treatment affected the mechanical and corrosion properties of the material.
- The microstructure changed by heat treatment resulted in enhanced corrosion resistance and mechanical properties.
- Corrosive environments had significant effects on corrosion resistance. The corrosion resistance of samples heat-treated in air and oil media was better than that of samples treated in a water medium.
- The electrochemical results showed that the heat-treated SS316L sample in oil exhibited the lowest passive current density, whereas the current density in water was highest in all solutions. Weight loss and surface roughness increased in all samples kept in different corrosive environments.
- Smooth surfaces provided superior corrosion protection. Corrosive environments increased the surface roughness and decreased the corrosion resistance. Especially in the tests performed in an SBF solution, corrosion occurred faster given the high HCl concentration.
- The heat treatment reduced the metal dissolution of the alloy through the formation of an oxide layer on the heat-treated steel surface or through stifling the removal of metallic ions via complex ion formation.
- Experimental studies illustrated that heat-treated stainless steel could demonstrate effectiveness in acidic environments because the corrosion behavior of stainless steel was similar with and without heat treatment. However, the corrosion susceptibility of heat-treated stainless steel was higher than that of nonheated stainless steel in alkaline and neutral media.
- Stainless steel manufacturers must understand the effect of cooling media to optimize corrosion resistance, and this work could be applied to many industrial areas using stainless steel, especially in the field of biomaterials.

Conflict of interest

The authors have no conflicts of interest to declare.

References

[1] M. P. Groover, *Fundamentals of Modern Manufacturing: Materials, Processes, and Systems*, John Wiley & Sons (2020).

[2] J. L. Del Abra-Arzola et al., Study of the effect of sigma phase precipitation on the sliding wear and corrosion behaviour of duplex stainless steel AISI 2205, *Wear,* 400 (2018) 43-51.

[3] G. Özer, Investigation of the effects of heat treatment conditions on phase change, hardness and corrosion behavior in the 1.4462 (AISI 2205) duplex stainless steel, *Niğde Ömer Halisdemir University Journal of Engineering Sciences,* 10 (1) (2021) 426-431.

[4] S. Virtanen, I. Milošev, E. Gomez-Barrena, R. Trebše, J. Salo and Y. T. Konttinen, Special modes of corrosion under physiological and simulated physiological conditions, *Acta Biomater.,* 4 (3) (2008) 468-476.

[5] C. Köse and R. Kaçar, Effect of welding speed on the mechanical properties and microstructure of laser welded AISI 316l stainless steel, *Journal of the Faculty of Engineering and Architecture of Gazi University*, 30 (2) (2015) 225-235.

[6] H. E. Emre, R. Kaçar A. Bülbül and B. Manisalı, Weldability of dissimilar AISI 316L-AISI 2205 stainless steel couple, *Omer Halisdemir University Journal of Engineering Sciences*, 6 (1) (2017) 244-256.

[7] M. Koyama, E. Akiyama, T. Sawaguchi, K. Ogawa, I. V. Kireeva, Y. I. Chumlyakov and K. Tsuzaki, Hydrogen-assisted quasi-cleavage fracture in a single crystalline type 316 austenitic stainless steel, *Corros. Sci.,* 75 (2013) 345-353.

[8] J. H. Shin and J. W. Lee, Effects of twin intersection on the tensile behavior in high nitrogen austenitic stainless steel, *Mater. Charact.*, 91 (2014) 19-25.

[9] M. Metikoš-Huković, Z. Pilić, R. Babić and D. Omanović, Influence of alloying elements on the corrosion stability of CoCrMo implant alloy in Hank's solution, *Acta Biomater.*, 2 (6) (2006) 693-700.

[10] F. Yıldız, A. Yetim and A. Çelik, The effect of temperature plasma nitriding on wear and magnetic properties of 316L implant material, *Suleyman Demirel University Journal of Engineering Sciences and Design,* 2 (3) (2014) 319-326.

[11] M. Niinomi, Metallic biomaterials, *J. Artif Organs*, 11 (3) (2008) 105-110.

[12] R. Nishimura and Y. Maeda, SCC evaluation of type 304 and 316 austenitic stainless steels in acidic chloride solutions using the slow strain rate technique, *Corros. Sci.,* 46 (3) (2004) 769-785.

[13] R. K. Singh Raman and W. H. Siew, Stress corrosion cracking of an austenitic stainless steel in nitrite-containing chloride solutions, *Materials,* 7 (2014) 7799-7808.

[14] J. J. Xie, H. Ningyu, X. Sun and J. Y. Zhan, Corrosion behavior of 316L stainless steel under Cl-corrosion medium, *IOP Conference Series: Materials Science and Engineering*, 711 (1) (2020) 012058.

[15] K. K. Chew, S. H. S. Zein and A. L. Ahmad, The corrosion scenario in human body: stainless steel 316L orthopaedic implants, *Natural Science,* 4 (3) (2012) 184-188.

[16] D. Gopi, V. C. A. Prakash and L. Kavitha, Evaluation of hydroxyapatite coatings on borate passivated 316L SS in Ringer's solution, *Mater. Sci. Eng., C,* 29 (3) (2009) 955-958.
[17] U. Kamachimudali, T. M. Sridhar and B. Raj, Corrosion of bio implants, *Sadhana*, 28 (2003) 601-637.
[18] T. M. Sridhar, U. K. Mudali and M. Subbaiyan, Preparation and characterisation of electrophoretically deposited hydroxyapatite coatings on type 316L stainless steel, C*orros. Sci.,* 45 (2) (2003) 237-252.
[19] I. Gurappa, Development of appropriate thickness ceramic coatings on 316 L stainless steel for biomedical applications, *Surf. Coat. Technol.,* 161 (1) (2002) 70-78.
[20] Y. Okazaki and E. Gotoh, Comparison of metal release from various metallic biomaterials in vitro, *Biomaterials*, 26 (1) (2005) 11-21.
[21] T. Tüken, Polypyrrole films on stainless steel, *Surf. Coat. Technol.,* 200 (16-17) (2006) 4713-4719.
[22] A. Parsapour, S. N. Khorasani and M. H. Fathi, Effect of surface treatment and metallic coating on corrosion behavior and biocompatibility of surgical 316L stainless steel implant, *J. Mater. Sci. Technol.,* 28 (2) (2012) 125-131.
[23] F. Kakaa and M. Ferkhi, In vitro corrosion study by EIS of stainless steel for orthopaedic applications, *Proceedings of the Third International Symposium on Materials and Sustainable Development* (2018) 301-305.
[24] N. Eliaz, Corrosion of metallic biomaterials: a review, *Materials,* 12 (3) (2019) 407.
[25] H. Aydin and A. Bayram, Determination of loss in mechanical properties of 2024 aluminum alloys in different heat-treated-state after corrosion, *Uludağ University Journal of The Faculty of Engineering,* 15 (1) (2010).
[26] M. M. Zerankeshi, R. Alizadeh, E. Gerashi, M. Asadollahi and T. G. Langdon, Effects of heat treatment on the corrosion behavior and mechanical properties of biodegradable Mg alloys, *J. Magnesium Alloys*, 10 (7) (2022) 1737-1785.
[27] O. Sinha, M. Talha and C. K. Behera, Potentiodynamic polarization study of type316L and 316LVM stainless steels for surgical implants in simulated body fluid, *Journal of Chemical and Pharmaceutical Research,* 4 (2012) 203-208.
[28] M. Yazıcı, O. Çomaklı, T. Yetim, A. F. Yetim and A. Çelik, The effect of plasma nitriding temperature on the electrochemical and semiconducting properties of thin passive films formed on 316 L stainless steel implant material in SBF solution, *Surf. Coat. Technol.,* 261 (2015) 181-188.
[29] A. Almubarak, W. Abuhaimed and A. Almazrouee, Corrosion behavior of the stressed sensitized austenitic stainless steels of high nitrogen content in seawater, *Int. J. Electrochem.,* (2013) 1-7.
[30] V. S. Raja and T. Shoji, *Stress Corrosion Cracking: Theory and Practice*, Elsevier (2011).
[31] N. A. Abd Razak, Y. P. Asmara and M. K. Kamaruzaman, Influences of H2SO4 and NaCl concentrations on stress corrosion cracking of AISI 304 stainless steel, *Advanced Materials Research*, 893 (2014) 410-414.
[32] P. L. Andresen, G. M. Gordon and S. C. Lu, The stress-corrosion-cracking model for high-level radioactive-waste packages, *JOM*, 57 (2005) 27-30.
[33] Y. Zhang, S. Wu and F. Cheng, A specially-designed super duplex stainless steel with balanced ferrite: austenite ratio fabricated via flux-cored wire arc additive manufacturing: microstructure evolution, mechanical properties and corrosion resistance, *Mater. Sci. Eng. A,* 854 (2022) 143809.
[34] K. Tippey, P. Jablonski, Ö. Doğan, J. Almer, R. Hackenberg, J. Speer, A. Stebner, K. Clarke, A. Clarke and K. Findley, Effects of alloying and processing modifications on precipitation behavior and elevated temperature strength in 9 % Cr ferritic/martensitic steels, *Mater. Sci. Eng. A,* 756 (2019) 172-183.
[35] Y. H. Kim, D. J. Lee, J. C. Byun, K. H. Jung, J. I. Kim, H. J. Lee, Y. T. Shin, S. H. Kim and H. W. Lee, The effect of sigma phases formation depending on Cr/Ni equivalent ratio in AISI 316L weldments, *Mater. Des.,* 32 (1) (2011) 330-336.
[36] M. O. H. Amuda and S. Mridha, Grain refinement and hardness distribution in cryogenically cooled ferritic stainless steel welds, *Mater. Des.,* 47 (2013) 365-371.
[37] K. Ceyhun and C. Topal, Influence of heat treatment on microstructure and mechanical properties of plasma arc welded AISI 410S ferritic stainless steel, *European Journal of Science and Technology* (19) (2020) 201-212.
[38] J. C. Lippold and D. J. Kotecki, *Welding Metallurgy and Weldability of Stainless Steels*, Wiley (2005).
[39] M. B. Krautkramer, Nondestructive material testing with ultrasonics-introduction to the basic principles, *The E-Journal of Nondestructive Testing and Ultrasonics,* 5 (2000) 11-27.
[40] M. Shirdel, H. Mirzadeh and M. Habibi Parsa, Microstructural evolution during normal/abnormal grain growth in austenitic stainless steel, *Metallurgical and Materials Transactions A*, 45 (2014) 5185-5193.
[41] S. Şenel, O. Koçar, E. Kocaman and O. Özdamar, Investigation of the mechanical and microstructural properties of AISI 430 steels after deep chryonegic treament, *European Journal of Science and Technology* (32) (2021) 1000-1005.
[42] F. Z. Xuan, X. Huang and S. T. Tu, Comparisons of 30Cr2Ni4MoV rotor steel with different treatments on corrosion resistance in high temperature water, *Materials & Design,* 29 (8) (2008) 1533-1539.
[43] Z. C. Li, H. Ding, R. D. K. Misra and Z. H. Cai, Microstructure-mechanical property relationship and austenite stability in medium-Mn TRIP steels: the effect of austenite-reverted transformation and quenching-tempering treatments, *Mater. Sci. Eng. A,* 682 (2017) 211-219.
[44] G. Argandoña, J. F. Palacio, C. Berlanga, M. V. Biezma, P. J. Rivero, J. Peña and R. Rodriguez, Effect of the temperature in the mechanical properties of austenite, ferrite and sigma phases of duplex stainless steels using hardness, microhardness and nanoindentation techniques, *Metals*, 7 (6) (2017) 219.
[45] C. Zhou, J. Wang, S. Hu, H. Tao, B. Fang, L. Li, J. Zheng and L. Zhang, Enhanced corrosion resistance of additively manufactured 316L stainless steel after heat treatment, *J. Electrochem. Soc.,* 167 (14) (2020) 141504.
[46] M. F. De Romero, Z. Duque, O. T. De Rincon, O. Pérez, I.

Araujo and B. Briceño, Microbiological corrosion: hydrogen permeation and sulfate-reducing bacteria, *Corrosion,* 58 (5) (2002) 429-435.

[47] R. Sundar, P. Ganesh, B. Sunil Kumar, R. K. Gupta, D. C. Nagpure, R. Kaul, K. Ranganathan, K. S. Bindra, V. Kain, S. M. Oak and B. Singh, Mitigation of stress corrosion cracking susceptibility of machined 304L stainless steel through laser peening, *J. Mater. Eng. Perform.,* 25 (2016) 3710-3724.

[48] Q. Hu, G. Zhang, Y. Qiu and X. Guo, The crevice corrosion behaviour of stainless steel in sodium chloride solution, *Corros. Sci.,* 53 (12) (2011) 4065-4072.

[49] B. Pradhan, Corrosion behavior of steel reinforcement in concrete exposed to composite chloride–sulfate environment, *Constr. Build. Mater.,* 72 (2014) 398-410.

[50] M. Cieślik, W. Reczyński, A. M. Janus, K. Engvall, R. P. Socha and A. Kotarba, Metal release and formation of surface precipitate at stainless steel grade 316 and Hanks solution interface-Inflammatory response and surface finishing effects, *Corros. Sci.,* 51 (5) (2009) 1157-1162.

[51] F. R. García-Galvan, S. Fajardo, V. Barranco and S. Feliu Jr, Experimental apparent stern–geary coefficients for AZ31B Mg alloy in physiological body fluids for accurate corrosion rate determination, *Metals,* 11 (3) (2021) 391.

[52] Y. C. Tang, S. Katsuma, S. Fujimoto and S. Hiromoto, Electrochemical study of type 304 and 316L stainless steels in simulated body fluids and cell cultures, *Acta Biomater.*, 2 (6) (2006) 709-715.

[53] H. Erbiyik, Definition of maintenance and maintenance types with due care on preventive maintenance, *Maintenance Management-Current Challenges, New Developments, and Future Directions*, IntechOpen (2022).

[54] A. F. Candelaria and C. E. Pinedo, Influence of the heat treatment on the corrosion resistance of the martensitic stainless steel type AISI 420, *J. Mater. Sci. Lett.,* 22 (16) (2003) 1151-1153.

[55] N. Arivazhagan, S. Singh, S. Prakash and G. M. Reddy, Hot corrosion studies on dissimilar friction welded low alloy steel and austenitic stainless steel under chlorine containing salt deposits under cyclic conditions, *Corros. Eng. Sci. Technol.,* 44 (5) (2009) 369-380.

[56] J. D. Fritz, Effects of metallurgical variables on the corrosion of stainless steels, *ASM Handbook Volume 13A. Corrosion: Fundamentals, Testing, and Protection*, ASM International (2003) 266-274.

[57] H. Y. Ma, C. Yang, G. Y. Li, W. J. Guo, S. H. Chen and J. L. Luo, Influence of nitrate and chloride ions on the corrosion of iron, *Corrosion*, 59 (12) (2003).

[58] S. Ghosh and V. Kain, Microstructural changes in AISI 304L stainless steel due to surface machining: effect on its susceptibility to chloride stress corrosion cracking, *J. Nucl. Mater.*, 403 (1-3) (2010) 62-67.

[59] X. He, R. G. Song and D. J. Kong, Microstructure and corrosion behaviour of laser-cladding Al-Ni-TiC-CeO2 composite coatings on S355 offshore steel, *J. Alloys Compd.,* 770 (2019) 771-783.

[60] U. Matik, Corrosion resistance of electroless NiP/NiB duplex coating, *UDCS'19 Fourth International Iron and Steel Symposium*, Karabuk, Türkiye (2019) 10-12.

[61] Z. E. Sánchez-Hernández, M. A. Dominguez-Crespo, A. M. Torres-Huerta, E. Onofre-Bustamante, J. Andraca Adame and H. Dorantes-Rosales, Improvement of adhesion and barrier properties of biomedical stainless steel by deposition of YSZ coatings using RF magnetron sputtering, *Mater. Charact.*, 91 (2014) 50-57.

[62] Z. Cvijović and G. Radenković, Microstructure and pitting corrosion resistance of annealed duplex stainless steel, *Corros. Sci.,* 48 (12) (2006) 3887-3906.

[63] S. Y. Lu, K. F. Yao, Y. B. Chen, M. H. Wang, X. Liu and X. Ge, The effect of tempering temperature on the microstructure and electrochemical properties of a 13 wt% Cr-type martensitic stainless steel, *Electrochim. Acta*, 165 (2015) 45-55.

[64] A. N. Isfahany, H. Saghafian and G. Borhani, The effect of heat treatment on mechanical properties and corrosion behavior of AISI420 martensitic stainless steel, *J. Alloys Compd.,* 509 (9) (2011) 3931-3936.

[65] T. Hryniewicz, R. Rokicki and K. Rokosz, Corrosion and surface characterization of titanium biomaterial after magnetoelectropolishing, *Surf. Coat. Technol.*, 203 (10-11) (2009) 1508-1515.

[66] S. Ghosh, V. P. S. Rana, V. Kain, V. Mittal and S. K. Baveja, Role of residual stresses induced by industrial fabrication on stress corrosion cracking susceptibility of austenitic stainless steel, *Materials & Design*, 32 (7) (2011) 3823-3831.

[67] L. Tóth, F. Haraszti and T. Kovács, Surface roughness effect in the case of welded stainless steel corrosion resistance, *Acta Materialia Transylvanica*, 1 (1) (2018) 53-56.



Şakir Altınsoy obtained his mechanical engineering B.Sc. from Mosul University, M.Sc. from Gazi University, and Ph.D. from Istanbul University. Since 2020, he has been working as an Assistant Professor at Istanbul Yeni Yüzyıl University.